Winner-Takes-All Dynamics and Antiphase States in Modulated Multimode Lasers

Kenju Otsuka
NTT Basic Research Laboratories, Musashino-shi, Tokyo, 180, Japan
(Received 18 March 1991)

$(N-1)!$ coexisting antiphase states are predicted to appear in an N-mode laser when the pump power drops below the threshold during part of the modulation cycle. The total output exhibits the so-called spiking mode pulsations at a frequency ω_s. However, each longitudinal-mode output shows pulses at a frequency ω_s/N, with each oscillator shifted by $2\pi/\omega_s$ from its neighbor, resulting from a "winner-takes-all" dynamics. The assignment to antiphase states embedded in a high-dimensional phase space by injection seeding is shown. Applicability to a rewritable memory of $(N-1)!$ different "dynamical patterns" is demonstrated on the basis of numerical simulations.

PACS numbers: 42.50.Tj, 02.90.+p, 05.45.+b

The issue of intensity fluctuation in the output of lasers was initiated by the pioneering work of McCumber [1]. His linear-response theory predicted a noise peak in power spectra corresponding to the relaxation oscillations in class-B lasers, in which polarization dynamics can be adiabatically eliminated. Such a frequency response was confirmed in semiconductor lasers [2] and solid-state lasers with a small periodic perturbation [3,4]. In the case of deep modulations of class-B lasers, the amplitude fluctuation changes drastically [5]. Klische, Telle, and Weiss demonstrated the period-doubling transition to chaotic relaxation oscillations in a deeply modulated NdP_5O_{14} solid-state laser in a modulation frequency regime near the relaxation frequency [6]. On the other hand, Kubodera and Otsuka investigated precisely the response of laser-diode-pumped $LiNdP_4O_{12}$ (LNP) lasers to a deep sinusoidal modulation of the pump intensity [4]. They found that periodic pulse oscillations (spiking mode) occur in a wide modulation frequency regime below the relaxation oscillation frequency whenever the pump power drops below the threshold during part of the cycle [4]. They also observed alternative spiking oscillations resulting from the cross-saturation effect in a deeply pump-modulated orthogonally dual-polarized LNP laser and reproduced the experiment surprisingly well on the basis of Tang-Statz-deMars's multimode rate equation model, which incorporates the spatial hole-burning effect [7]. In their observation, each lasing mode exhibits alternative pulse trains at every other modulation cycle of the spiking mode frequency.

Similar problems featuring the interaction between degrees of freedom have been investigated in several nonlinear systems [8,9]. Wiesenfeld *et al.* recently observed the so-called antiphase state, which was first predicted for Josephson-junction arrays [10], in intracavity second-harmonic generation in a multimode yttrium-aluminum-garnet laser [11]. Such a state is periodic in time, with each lasing mode having the same wave form. However, each oscillator is shifted by $1/N$ of a period from its neighbor, i.e., $I_k(t)=I_0(t+Tk/N)$, $k=1,2,\ldots,N$, where I_0 is a wave form of period T. This implies the simultaneous existence of $(N-1)!$ attractors in the phase space. Therefore, such systems which possess antiphase states are fascinating candidates for investigating complex dynamics involving an extremely large number of coexisting attractors.

The alternative spiking pulsation of Kubodera and Otsuka [4] strongly suggests the simplest (1,1) antiphase state [11]. This raises the question, *"What kind of spiking oscillation takes place when the oscillating mode number N increases?"* If N alternative spiking states, or rather antiphase states, do exist in deeply modulated N-mode lasers, such a system will provide another example for investigating the dynamics of coexisting attractor systems.

With this motivation, in this Letter we investigate the response of class-B multimode lasers to a deep sinusoidal pump modulation theoretically, paying special attention to an interplay between lasing modes. As normalized multimode rate equations [12], the following coupled N-mode equations are obtained [4,7]. These equations are universally applicable to homogeneously broadened class-B lasers with spatial hole burning and may be modified to include globally coupled laser arrays. Indeed, almost all solid-state lasers belong to this category, since the spatial diffusion of population is slow enough to create spatial holes:

$$dn_0/dt = w - n_0 - \sum_{k=1}^{N} \Gamma_{g,k}(n_0 - n_k/2)s_k , \tag{1}$$

$$dn_k/dt = \Gamma_{g,k} n_0 s_k - n_k \left(1 + \sum_{k=1}^{N} \Gamma_{g,k} s_k\right) , \tag{2}$$

$$ds_k/dt = K\{[\Gamma_{g,k}(n_0 - n_k/2) - \Gamma_{l,k}]s_k + \epsilon_k n_0 + s_{i,k}\}, \quad k=1,2,\ldots,N , \tag{3}$$

where $t=T/\tau$ is the normalized time (τ is the population lifetime), w is the pump power normalized by the first lasing mode threshold, n_0 is the constant term of the spatial Fourier expansion of the population inversion density due to spatial hole burning normalized by the first lasing mode threshold, n_k is the first-order Fourier component of population inversion density for the kth mode, s_k is the normalized photon density, $\Gamma_{g,k}$ is the emission cross-

section (gain) ratio to the first lasing mode, $\Gamma_{l,k}$ is the loss ratio to the first lasing mode, $K=\tau/\tau_p$ (τ_p is the photon lifetime), and ϵ_k is the spontaneous emission rate for the kth mode. Here, $s_{i,k}$ is an "injection-seed" signal, which will be discussed later. Note that each lasing mode globally couples with all other modes through cross saturation of population inversion.

In the following analysis, we assume for brevity that the gain spectrum is wide enough as compared with longitudinal mode spacing, and the gain, loss, and spontaneous emission rate are the same for all modes. The following results are generally obtained if effective gains are the same for all lasing modes, i.e., $\Gamma_{g,k}=\Gamma_{l,k}$ [13].

An N-mode free-running laser is always stable in time and the relaxation oscillations are damped out. The relaxation oscillation frequency for N-mode free-running lasers coincides with that of a single-mode laser, which is derived from the linear stability analysis as [12]

$$\omega_r=[(\tfrac{3}{2}\bar{n}_0-\bar{n}_1)\bar{s}_1/\tau\tau_p]^{1/2}. \tag{4}$$

Here, $\bar{n}_0$, $\bar{n}_1$, and $\bar{s}_1$ are the stationary values for $N=1$. This is exactly the same value as $\omega_r=[(w-1)/\tau\tau_p]^{1/2}$, which is obtained from McCumber's linearized theory [1].

For a small modulation depth, i.e., $w_0>1$ and $\Delta w\ll w_0-1$ in $w(t)=w_0+\Delta w\cos(\tau\omega_m t)$, only *resonant relaxation oscillations* [4] are observed around $\omega_m=\omega_r$. If modulation depth increases such that the pump power drops below the threshold during part of the cycle (i.e., $\Delta w>w_0-1$), the spiking mode oscillations, which appear as a repetitive generation of the first peak in the onset of relaxation oscillations, take place in a wide region below the relaxation oscillation frequency ω_r. The lowest repetition frequency edge of the spiking mode (optimum spiking mode frequency), at which the highest peak power is obtained, is given by [4]

$$\omega_{s,\mathrm{opt}}=\pi[2\ln(2\epsilon\sqrt{K})^{-1}]^{-1/2}\times[(w_0-1)/(w_m-1)]^{1/2}\omega_r, \tag{5}$$

according to Carlson's procedure [14], where $w_m=w_0+(2/\pi)\Delta w$ denotes the pulse height of an equivalent rectangular pump pulse [4]. The observed spiking mode frequency in a diode-pumped LNP laser coincided satisfactorily with Eq. (5); furthermore, alternative spiking mode oscillations for $N=2$ dual-polarization oscillations were reproduced surprisingly well by the numerical simulation of Eqs. (1)–(3) [4].

When initial conditions for all the lasing modes are exactly the same, the highest peak-power spiking mode takes place at the frequency $\omega_{s,\mathrm{opt}}$ given by Eq. (5). In this case, each lasing mode produces *synchronized* spiking output. Needless to say, however, such a *synchronized* spiking mode can never be realized in the real experiment. Indeed, if one introduces an extremely small perturbation to initial conditions, synchronization fails and each mode exhibits separate spiking pulsations. The simplest example for $N=2$ is shown in Fig. 1, where $w_0=2.7$, $\Delta w=2$, $K=10^3$, and $\epsilon=1.2\times10^{-7}$ are assumed [4]. Note that each mode alternatively produces periodic spikes at the frequency $\frac{1}{2}\omega_s$ and the total output exhibits the spiking mode at the frequency of ω_s.

The mechanism of the alternative spike pulse oscillation can be explained as follows. The time delay for the spike mode is given by the buildup time of the population inversion $n_0-n_k/2$ to reach the threshold value, plus the growth time of the photon density s_k after the population density exceeds the threshold. For the first pump cycle in Fig. 1, the first mode $k=1$ reaches the threshold first, and the second mode oscillation is suppressed due to the cross saturation, i.e., quenching. On the other hand, the stepwise decrease in $n_0-n_1/2$ resulting from the self-saturation, just after the oscillation of s_1, is more significant than that in $n_0-n_2/2$. Thus, the recovery time of the population inversion to its threshold value is shorter for the second mode than for the first mode, and the second mode (s_2) oscillation builds up and suppresses the first mode during the next pump cycle. (It should be noted that the pulse height is lower than for the $N=1$ case resulting from the cross-saturation effect. This results in an increase in the optimum spiking mode frequency for antiphase states. In general, the optimum spiking mode frequency increases as N increases.)

Do such alternative spiking pulsations take place for larger N values? As for small N, the alternative spiking mode is indeed excited. In short, the total output exhibits spiking mode oscillations at the frequency of ω_s and each oscillator produces N alternative pulses at the frequency of ω_s/N. An example for $N=3$ is shown in Fig. 2(c). This is nothing more than the antiphase state. The antiphase states are globally attracting and are observed for arbitrary initial conditions. There coexist $(N-1)!$ antiphase periodic attractors in the phase space. Which antiphase state is attained depends on the initial conditions. For modulation below the optimum spiking frequency [i.e., region A in Fig. 2(a)], chaotic spiking oscillations

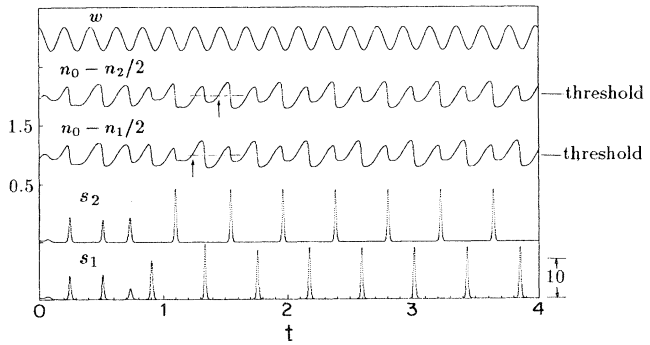

FIG. 1. Computer analysis for $N=2$ alternative spiking oscillations.

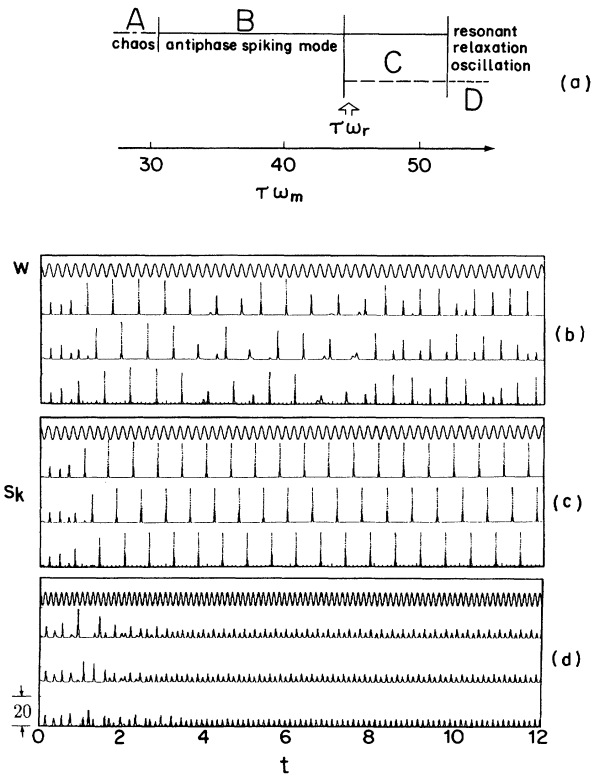

FIG. 2. (a) Typical frequency response diagram. $N=3$, $w_0=3$, $K=10^3$, $\epsilon=1.2\times10^{-7}$, and $\Delta w=2.3$ are assumed. Such a scenario always exists independently of N. (b) Chaotic spiking oscillation in region A. $\tau\omega_m=30$. (c) Antiphase spiking mode oscillation in region B. $\tau\omega_m=32$. (d) Alternative pulsation of spiking mode and resonant relaxation oscillation in region C. $\tau\omega_m=50$. The so-called *clustering* [8] is occurring in this region.

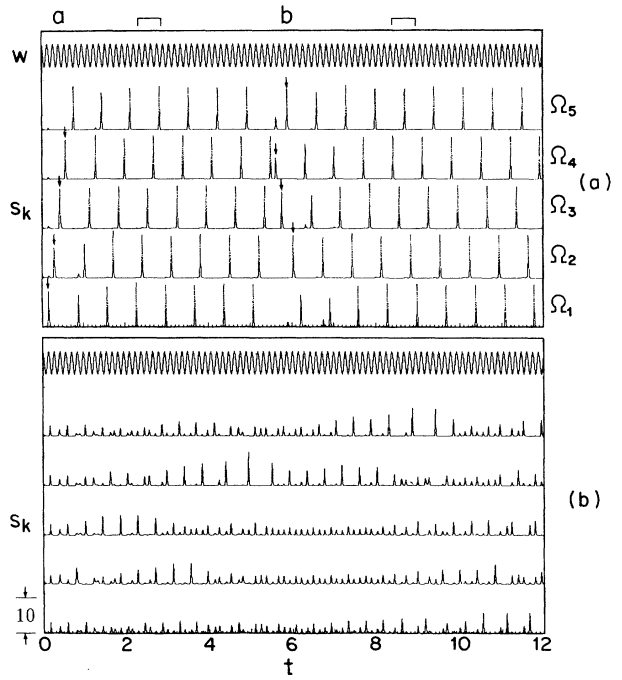

FIG. 3. Assignment to desired antiphase states by "seeding." $N=5$, $w_0=3$, $\Delta w=2.3$, and $\tau\omega_m=45$. Seed pulse intensity: $s_{i,k}=0.2$ [$\approx$ (laser pulse height)/60]; pulse width: $\Delta t=0.06$. (a) With seeding and (b) without seeding.

occur as shown in Fig. 2(b). As ω_m increases up to region C, various attractors such as suggested by the wave forms in Fig. 2(d) tend to coexist with antiphase spiking states. (The total output wave form for this particular attractor well corresponds to the alternative spike pulses of the spiking mode and the resonant relaxation oscillation which was observed in the Kubodera-Otsuka experiment [4].) However, these attractors have narrow basins of attraction and the system is predominantly attracted to the antiphase states. As ω_m increases further, *synchronized* sustained resonant relaxation oscillations are excited in region D. A quite similar frequency response, featuring A, B, C, and D regions, was obtained experimentally in the single-mode laser [see Fig. 2(a) in Ref. [4]].

When N increases with a decrease in mode spacing, the basins of attraction of antiphase states become increasingly close packed ("attractor crowding" [15]) and shrink rapidly. In the present system, consequent to the shrinkage of the basins of attraction of antiphase states, regions C and D in Fig. 2(a) spread and other attractors like those in Fig. 2(d), as well as resonant relaxation oscillations, which have increased basins of attraction, tend to coexist with the antiphase states with multiplicity. Consequently, antiphase states can rarely be attained for arbitrary initial conditions. Furthermore, the lower the symmetry, i.e., $\Gamma_{g,k}\neq\Gamma_{l,k}$, the greater the multiplicity.

However, if the system size is not extremely large, such multiplicity can be overcome by the following "seeding" method and one can assign the system to desired antiphase states. Inject light pulses to $N-1$ modes in the desired sequences as seeds at the time interval of $2\pi/\omega_r$ only during the $N-1$ modulation cycle. Then, the seeded mode builds up first and other modes are quenched similarly to Fig. 1 (*winner-takes-all dynamics* [16]). The desired dynamic "firing" pattern then persists, repeating with the time interval of $2N\pi/\omega_s$. The result is shown in Fig. 3(a) for $N=5$, where seed light pulses are injected to lasing modes oscillating at frequencies Ω_k, with the sequence $\Omega_1\rightarrow\Omega_2\rightarrow\Omega_3\rightarrow\Omega_4$ in region a, and $\Omega_4\rightarrow\Omega_3\rightarrow\Omega_5\rightarrow\Omega_2$ in region b. Even for $N=5$, 24 antiphase states coexist, together with other attractors. However, with seeding, the desired antiphase state possessing the same dynamic firing pattern as the seed, repeating at the period $2n\pi/\omega_s$ indicated by the brackets at the top of the figure, is successfully excited, and even switching (see region b) is possible. In other words, dynamic memory embedded in a high-dimensional phase space is recalled by the triggering seed. The seeding condition for realizing antiphase states in terms of pulse height and pulse width

is not so severe. Without seeding under the same initial conditions as Fig. 3(a), chaotic motion persists and the system can hardly find antiphase attractors, as shown in Fig. 3(b). From the applications point of view, the present seeding experiment implies that the present antiphase states can be utilized, in principle, to perform rewritable memory operations on $(N-1)!$ different "dynamic patterns." Similar dynamic memory operations employing seeding methods have been reported in different contexts [16,17].

When N increases further, however, extraordinary multiplicity might possibly result in the noise-induced escape from antiphase attractors [15]. Another interesting question arises as to whether the self-induced switching-path formation (*chaotic itinerancy* [18]) among destabilized patterns occurs in the present system for a large-N limit. The quantitive evaluation of basins of attraction of coexisting attractors, phase-space landscape featuring connectivities between antiphase states, and sensitivity to external noise would be a future problem for understanding the complex dynamics involving an extraordinarily large number of coexisting antiphase states.

[1] D. E. McCumber, Phys. Rev. **141**, 306 (1966).
[2] T. Ikegami and Y. Suematsu, IEEE J. Quantum Electron. **4**, 148 (1968).
[3] T. Kimura and K. Otsuka, IEEE J. Quantum Electron. **6**, 764 (1970).
[4] K. Kubodera and K. Otsuka, IEEE J. Quantum Electron. **17**, 1139 (1981).
[5] H. G. Danielmeyer and F. W. Ostermayer, J. Appl. Phys. **43**, 2911 (1972).
[6] W. Klische, H. R. Telle, and C. O. Weiss, Opt. Lett. **9**, 561 (1984).
[7] C. L. Tang, H. Statz, and G. deMars, J. Appl. Phys. **34**, 2289 (1963).
[8] K. Kaneko, Physica (Amsterdam) **41D**, 137 (1990).
[9] K. Y. Tsang and K. Wiesenfeld, Appl. Phys. Lett. **56**, 495 (1990).
[10] P. Hadley and M. R. Beasley, Appl. Phys. Lett. **50**, 621 (1987).
[11] K. Wiesenfeld, C. Bracikowski, G. James, and R. Roy, Phys. Rev. Lett. **65**, 1749 (1990).
[12] K. Otsuka and K. Kubodera, IEEE J. Quantum Electron. **16**, 419 (1980); K. Otsuka, *ibid.* **13**, 520 (1977).
[13] In experiments, this situation is realized by introducing a frequency-dependent loss element, such as specially coated laser mirrors or filters, into the cavity so as to compensate a gain distribution. This is feasible by means of the state-of-art coating technology. Here, parameter values of $\Gamma_{g,k}=\Gamma_{l,k}=1$ are assumed for all the calculations. However, the dynamics do not change whenever $\Gamma_{g,k}=\Gamma_{l,k}$ is satisfied for each mode even if a mode-dependent $\Gamma_{g,k}$ resulting from the gain distribution is introduced. It has also been confirmed for small N that the presence of a small effective gain asymmetry does not lead to the destruction of periodic antiphase attractors, although a quantitive measure of the size of the allowed symmetry should be clarified for various parameters (w, Δw, ω_m) and N.
[14] D. G. Carlson, J. Appl. Phys. **39**, 4369 (1968).
[15] K. Wiesenfeld and P. Hadley, Phys. Rev. Lett. **62**, 1335 (1989).
[16] D. Z. Anderson, C. Benkert, and A. Hermanns, in *Topical Meeting on Nonlinear Dynamics in Optical Systems, 1990,* Technical Digest Series (Optical Society of America, Washington, DC, 1990), p. 104.
[17] T. Aida and P. Davis, Jpn. J. Appl. Phys. **29**, L1241 (1990).
[18] K. Otsuka, Phys. Rev. Lett. **65**, 329 (1990); Phys. Rev. A **43**, 618 (1991).